Article

A new signal amplification strategy using semicarbazide as co-reaction accelerator for highly sensitive electrochemiluminescent aptasensor construction

Meng-Nan Ma, Ying Zhuo, Ruo Yuan, and Yaqin Chai

Anal. Chem., **Just Accepted Manuscript** • DOI: 10.1021/acs.analchem.5b02848 • Publication Date (Web): 12 Oct 2015

A new signal amplification strategy using semicarbazide as co-reaction accelerator for highly sensitive electrochemiluminescent aptasensor construction

Meng-Nan Ma, Ying Zhuo*, Ruo Yuan, Ya-Qin Chai*

Key Laboratory of Luminescent and Real-Time Analytical Chemistry (Southwest University), Ministry of Education, College of Chemistry and Chemical Engineering, Southwest University, Chongqing 400715,China.

Corresponding author. Tel.: +86-23-68252277; Fax: +86-23-68253172.

E-mail address: yingzhuo@swu.edu.cn (Y. Zhuo), yqchai@swu.edu.cn (Y.Q. Chai)

ABSTRACT

A highly sensitive electrochemiluminescent (ECL) aptasensor was constructed using semicarbazide (Sem) as co-reaction accelerator to promote the ECL reaction rate of CdTe quantum dots (CdTe QDs) and the coreactant of peroxydisulfate ($S_2O_8^{2-}$) for boosting signal amplification. The co-reaction accelerator is a species that when it is introduced into the ECL system containing luminophore and coreactant, it can interact with coreactant rather than luminophore to promote the ECL reaction rate of luminophore and coreactant, thus the ECL signal is significantly amplified in comparison with that in the only presence of luminophore and coreactant. In this work, the ECL signal probes were first fabricated by alternately assembling the Sem and Au nanoparticles (AuNPs) onto the surfaces of hollow Au nanocages (AuNCs) *via* Au-N bond to obtain the multi-layered nanomaterials of $(AuNPs\text{-}Sem)_n$-AuNCs for immobilizing amino-terminated detection aptamer of thrombin (TBA 2). Notably, the Sem with two $-NH_2$ terminal groups could not only serve as crosslinking reagent to assemble AuNPs and AuNCs but also act as co-reaction accelerator to enhance the ECL reaction rate of CdTe QDs and $S_2O_8^{2-}$ for signal amplification. With the sandwich-type format, TBA 2 signal probes could be trapped on the CdTe QD-based sensing interface in the presence of thrombin (TB) to achieve a considerably enhanced ECL signal in $S_2O_8^{2-}$ solution. As a result, the Sem in the TBA 2 signal probes could accelerate the reduction of $S_2O_8^{2-}$ to produce the more oxidant mediators of $SO_4^{\bullet-}$, which further boost the production of excited states of CdTe QDs to emit light. With the employment of the novel co-reaction accelerator Sem, the proposed ECL

biosensor exhibited ultrahigh sensitivity to quantify the concentration of TB from 1×10^{-7} nM to 1 nM with a detection limit of 0.03 fM, which demonstrated that the co-reaction accelerator could provide a simple, efficient, and low-cost approach for signal amplification and hold a great potential for other ECL biosensors construction.

KEYWORDS: Co-reaction accelerator, Signal amplification, Peroxydisulfate, Semicarbazide, CdTe quantum dots, Electrochemiluminescence aptasensor.

INTRODUCTION

Quantum dots (QDs), first reported with electrochemiluminescence (ECL) phenomenon by the Bard group in 2002,[1] have attracted considerable interests in basic research and clinical applications of QD-based ECL assay due to its size controlled luminescence, high quantum yield and stable light emission.[2,3,4] However, compared with conventional luminescent reagents,[5,6,7] such as ruthenium(II) tris(2,2'-bipyridyl) ($Ru(bpy)_3^{2+}$) and its derivatives, the luminescent efficiency of QDs was lower so that effective coreactants were introduced to enhance the ECL response.[1,8,9] It was reported that the possible ECL mechanism of peroxydisulfate ($S_2O_8^{2-}$) serving as the coreactant of QDs was as follows: $S_2O_8^{2-}$ was initially electrochemically reduced to produce the oxidant intermediates of $SO_4^{\bullet-}$, which could then react with the negatively-charged QDs by injecting a hole into the highest occupied moleculoar or bital to induce an excited state, leading to significant enhancement of ECL intensity.[10] Thus the larger amount of the mediators of $SO_4^{\bullet-}$ were produced, the stronger of the ECL response of QDs could be achieved. Admittedly, to increase the concentration of $S_2O_8^{2-}$ might be a feasible approach to improve the production of $SO_4^{\bullet-}$. However, due to the limited solubility of $S_2O_8^{2-}$ and non-absolutely linear relationship between the concentration of $S_2O_8^{2-}$ and the amount of $SO_4^{\bullet-}$, the ECL intensity enhancement was limited by just increasing the $S_2O_8^{2-}$ concentration. Therefore, if a kind of reagent could accelerate the reduction of $S_2O_8^{2-}$, resulting in the generation of more oxidant intermediates of $SO_4^{\bullet-}$, the amount of excited states of QDs could be increased to further amplify the ECL signal. In our experiment, the semicarbazide (Sem) was used to interact with $S_2O_8^{2-}$ to

promote the ECL reaction rate of QDs and $S_2O_8^{2-}$ ECL system for significantly boosting the ECL intensity. Therefore, the reagent that can interact with corectant rather than luminophore to improve the ECL reaction rate of luminophore and corectant is named as co-reaction accelerator.

With low density, large surface area and shell permeability, hollow nanostructures have been drawing intense research interest because of their widespread potentials in many areas, such as catalysis, energy storage/conversion, sensing and controlled delivery.[11] Among various hollow nanostructures, the hollow Au nanocages (AuNCs) have attracted the most attentions, for that the AuNCs not only possess highly specific surface areas and superior electron transport capacity, more importantly, they are more biocompatible and present a well-established surface for easy functionalization. Therefore, the AuNCs can serve as structural platforms for the construction of multifunctional materials.[12] In view of this, we first synthesized the cage-like nanostructures of AuNCs using galvanic replacement reactions with silver nanocubes as a template.[13] Subsequently, the prepared AuNCs were functionalized by Sem and Au nanoparticles (AuNPs) through layer-by-layer assembly to obtain the multi-layered nanomaterials of $(AuNPs\text{-}Sem)_n$-AuNCs for immobilizing a large number of amino-terminated detection thrombin aptamers (TBA 2) as signal probes. Notably, since abundant Sem as co-reaction accelerator was introduced into the TBA 2 signal probes, the ECL reaction rate of CdTe QDs and $S_2O_8^{2-}$ was promoted to enhance the ECL response for signal amplification.

Meanwhile, in this study, the CdTe QD-based sensing interface was constructed by

coating the CdTe QDs modified C_{60} nanoparticles (CdTe QDs@C_{60}NPs) on the glassy carbon electrode (GCE) which used chitosan (CS) as film-forming substrate. Then the Au nanopaticles (Dp AuNPs) were electrochemically deposited on the resultant electrode for thiol-terminated thrombin capture aptamer (TBA 1) loading. After TBA 1, thrombin (TB), and TBA 2 signal probes forming a sandwich-type structure, a considerably enhanced ECL signal was obtained in the $S_2O_8^{2-}$ solution, for that Sem in the TBA 2 signal probes could accelerate the reduction of $S_2O_8^{2-}$ to produce the more oxidant mediators of $SO_4^{\bullet-}$, which further boosted the production of excited states of QDs to emit light. Therefore, such ECL aptasensor based on the employment of Sem as co-reaction accelerator to promote the ECL reaction rate of CdTe QDs and $S_2O_8^{2-}$ could enhance the ECL efficiency and sensitivity of the CdTe QD-based ECL system.

The schematic illustration of ECL aptasensor preparation process and possible luminescence mechanism were shown in Scheme 1.

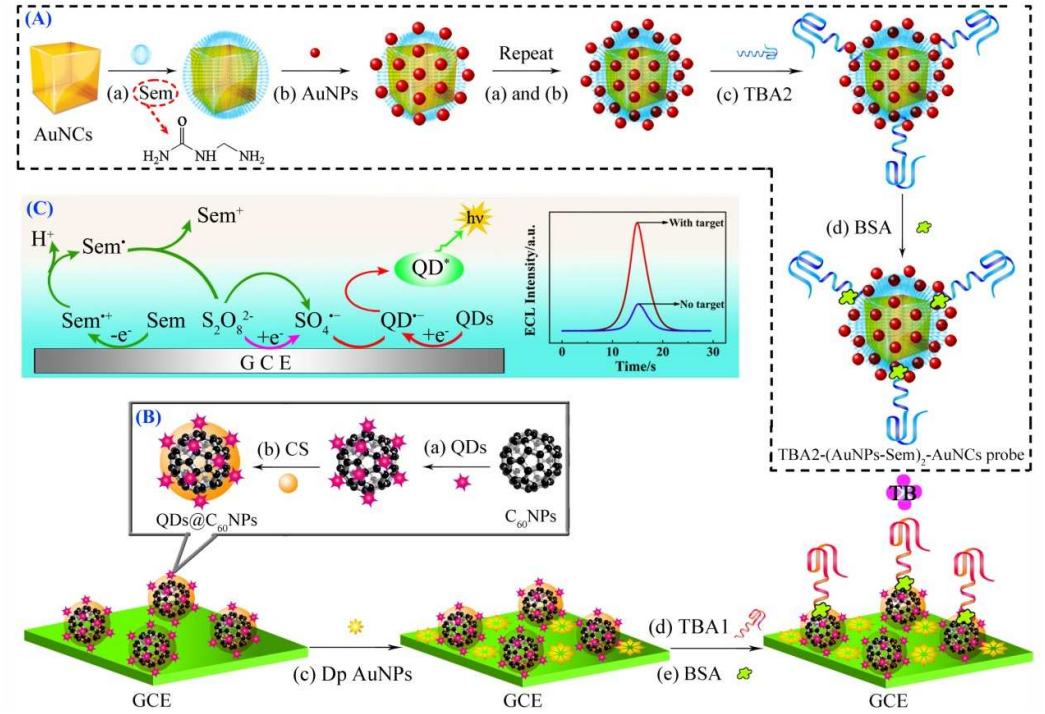

Scheme 1. Schematic illustration of ECL aptasensor preparation process and possible luminescence mechanism. (A) Fabrication of TBA 2-(AuNPs-Sem)$_n$-AuNCs signal probe; (B) Fabrication of CdTe QDs@C_{60} NPs and (C) the possible ECL mechanism of QD-based ECL system.

EXPERIMENTAL METHODS

Reagents and materials. Sem and silver nitrate ($AgNO_3$) were ordered from the Sinopharm Chemical Reagent Co., Ltd (Shanghai, China). Sodium sulfide (Na_2S) was received from Chongqing Boyi Chemical Reagent Co., Ltd (Chongqing, China). Poly (diallyldimethyl ammonium chloride) (PDDA, 20%, *w/w* in water), glutaraldehyde (GA, 25% *w/w* in water), 3-mercaptopropionic acid (MPA), CS ($\geqslant$ 75% deacetylation), TB, bovine serum albumin (BSA), human serum albumin (HSA), hemoglobin (Hb) and gold chloride ($HAuCl_4 \cdot 4H_2O$) were purchased from Sigma Chemical Co. (St. Louis, MO, USA). Fullerene C_{60} (99.5%) was obtained from Pioneer Nanotechnology Co. (Nanjing, China). Cadmium chloride hemipenta hydrate ($CdCl_2 \cdot 2.5H_2O$) and sodium tellurite (IV) (Na_2TeO_3) were received from Alfa Aesar Chemical Co., Ltd (Tianjin, China). Ethylene glycol (EG, 99.5%), poly(vinylpyrrolidone) (PVP), $NaBH_4$ and trisodium citrate dihydrate were obtained from Kelong Chemical Company (Chengdu, China). The sequence of TBA 1 (2.5 μM) and TBA 2 (2.5 μM) were

TBA 1: 5'-SH-GGTTGGTGTGGTTGG-3';

TBA 2: 5'-NH_2-AGTCCGTGGTAGGGCAGGTTGGGGTGACT-3'.

They were ordered from Shanghai Sangon Biological Engineering Technology and Services Co., Ltd. (Shanghai, China). $Na_2S_2O_8$ was bought from Chengdu Chemical Reagent Company (Chengdu, China). $[Fe(CN)_6]^{3-/4-}$ solution consisted of 10 mM $K_3Fe(CN)_6$, 10 mM $K_4Fe(CN)_6$, 0.1 M Na_2HPO_4, 0.1 M KH_2PO_4 and 0.1 M KCl. Phosphate buffer solution (PBS, pH 7.4) was prepared using 0.1 M Na_2HPO_4, 0.1 M

KH_2PO_4 and 0.1 M NaCl. 20 mM Tris-HCl buffer (pH 7.4) containing 140 mM NaCl, 5 mM KCl and 1 mM $MgCl_2$ was used as the dilution of aptamers. All other reagents were of analytical grade and were used as received. Deionized water was used throughout. C_{60}NPs[14] and AuNPs (51 nm diameter)[15] were prepared according to the reports.

Instrumentation. UV-vis spectra were obtained on a UV-2450 UV-vis spectrophotometer (Shimadzu, Tokyo, Japan). Photoluminescence (PL) spectra were collected with a RF-5301PC spectrophotometer (Shimadzu, Tokyo, Japan). The ECL emission and cyclic voltammetric (CV) measurements were monitored by a MPI-A electrocheminescence analyzer of the Xi'an Remax Electronicscience & Technology Co., Ltd (Xi'an, China), the working potential was -1.5~0 V or -2~0 V with the voltage of the photomultiplier tube (PTM) setting at 800 V and the rate of 100 mV/s in the process of detection. The electrochemical impedance spectroscopy (EIS) measurements were recorded on a CHI 660 D electrochemistry workstation of the Shanghai CH Instruments (Shanghai, China). A conventional three-electrode system, containing a modified GCE working electrode, a platinum counter electrode and an Ag/AgCl (saturated KCl solution) reference electrode, was used in the experiment. The morphologies of nanoparticles were characterized on a scanning electron microscope (SEM) on the Hitachi S-4800 Instrument (Tokyo, Japan) and a high resolution transmission electron microscope (HRTEM) on the JEM 1200EX Instrument (JEOL, Japan).

Preparation of CdTe QDs. CdTe QDs were synthesized according to the

previously reported methods with some modifications.[16] Firstly, the flask and stirrer were soaked in chromic acid solution overnight for cleaning. Then, 36.89 mg $CdCl_2$ was dissolved in 50 mL deionized water. Afterwards, 50 mg trisodium citrate dihydrate, 1 mL Na_2TeO_3 (0.01 M), 33 μL MPA and 100 mg $NaBH_4$ were added into the solution under stirring at room temperature. At last, the obtained solution was refluxed at 110 °C for 10 h. The resultant CdTe QDs were washed with ethanol and separated by centrifugation. The final product was dispersed in deionized water and stored at 4 °C until use.

Preparation of CdTe QDs@C_{60}NPs. Initially, 300 μL of the obtained C_{60}NPs (1 mg/mL) was added into 50 μL 0.2 % PDDA aqueous solution with the aid of ultrasonic agitation for 30 min to obtain the positively charged C_{60}NPs. Subsequently, the above materials was centrifuged and washed for twice by deionized water. Afterwards, 100 μL of the synthesized CdTe QDs (0.1 mg/mL) were added into the above mixture for 12 h under stirring, followed by centrifugation and dispersion in 10 μL of 0.05% CS solution (see Scheme 1B). The final product was stored at 4 °C until use.

Preparation of AuNCs. AuNCs were prepared according to the report with minor modification.[13] Initially, 3 mM Na_2S, 0.02 g/mL PVP and 282 mM $AgNO_3$ solutions were prepared by using EG solution as dispersion, respectively. Then 30 mL EG solution was heated at 150 °C for 1 h. Subsequently, 0.4 mL Na_2S solution was added into the hot EG solution, followed by adding 10 mL PVP solution and 3.5 mL $AgNO_3$ solution. After the color of the mixture changed from white to brown, the Ag

nanocubes were prepared. To remove the unreacted materials, the resultant product was diluted with acetone and washed with deionized water. Afterwards, the solution of purified Ag nanocubes was brought to a boil and 100 μL of 1% $HAuCl_4 \cdot 4H_2O$ solution was injected slowly. The mixture was continuously refluxed until its color changed from brown to pink. At last, the AuNCs were collected through centrifugation and the final product was stored at 4 °C when not used.

Preparation of TBA 2-(AuNPs-Sem)$_n$-AuNCs signal probe. Firstly, 200 μL Sem (10 mM) solution was added into the synthesized 500 μL AuNCs solution (1 mg/mL) for 12 h under stirring to obtain the Sem decorated AuNCs. After washed twice by deionized water, the dispersion was collected by centrifugation and dispersed in deionized water. Then, 200 μL of the prepared AuNPs solution (1 mg/mL) was added into the above solution with stirring for 12 h, followed by centrifuging and washing for several times by deionized water. Additional Sem and AuNPs layers could be attached by repeating the above procedure to achieve the multi-layered nanomaterials of (AuNPs-Sem)$_n$-AuNCs. Next, 200 μL of 2.5 μM TBA 2 solution was added with stirring for 12 h, which followed by washing with deionized water. At last, to block nonspecific binding sites, 50 μL of 0.25% BSA was added to the mixture for about 1 h and the prepared TBA 2 signal probe (TBA 2-(AuNPs-Sem)$_n$-AuNCs) was stored at 4 °C for further use (see Scheme 1A). In addition, three kinds of different TBA 2 signal probes were prepared for comparison and the detail preparation processes were listed in the Supporting Information.

The fabrication of the sandwich-type ECL aptasensor. A GCE (4 mm in

diameter) was first polished with 0.05 μm alumina powder. After successive sonication in deionized water, the cleaned electrode was allowed to dry in the air. Then the cleaned electrode was coated with 10 μL CdTe QDs@C_{60}NPs using CS as film-forming substrate and dried at room temperature to get a uniform composite film. Next, the modified electrode was immersed in $HAuCl_4 \cdot 4H_2O$ solution (1%) and electrochemically deposited at -0.2 V for 30 s to obtain the Dp AuNPs layer. Afterwards, 20 μL of 2.5 μM TBA 1 was dropped onto the surface of Dp AuNPs/CdTe QDs@C_{60}NPs layer for about 16 h. To block nonspecific binding sites, 20 μL of BSA (0.25%) was incubated with the resultant electrode for 40 min (see Scheme 1). The finished aptasensor was stored at 4 °C for further use.

The detection of the sandwich-type ECL aptasensor. Firstly, 20 μL standard solution of TB was coated on the prepared aptasensor for 40 min. Then 10 μL TBA 2 signal probes incubated with the resultant electrode for another 1 h. After the prepared aptasensor was washed with PBS, the ECL measurement was performed in $S_2O_8^{2-}$ solution (0.1 M, pH = 7.4). As expected, the changes of the ECL intensity ($\Delta I_{ECL} = I - I_0$, I was the ECL intensity of the aptasensor after immobilizing of TBA 2 signal probes and I_0 was the ECL intensity of the aptasensor before incubating with TB, respectively) linearly increased as the concentration of TB increased. Therefore, ΔI_{ECL} of the aptasensor was recorded for quantitative analysis of the TB.

RESULTS AND DISCUSSION

SEM and TEM characterization of the different nanomaterials. Firstly, in Figure 1A, we could see the HRTEM image of the CdTe QDs@C_{60}NPs composite, which showed that many dots were covered on the surface of the globular hollow structures. From the enlarged HRTEM mages (Figure 1B and C), the crystalline structure of CdTe QDs with the existence of well-resolved lattice planes was apparently observed on the surface of C_{60}NPs and the diameters of CdTe QDs were mainly distributed in the range of less than 5 nm, which provided direct evidence for the formation of CdTe QDs@C_{60}NPs. From Figure 1D, we could see the SEM image of C_{60}NPs with globular hollow structures and diameter of 42.1±4 nm, which were consistent with previous report.[17] Figure 1E showed the SEM image of AuNCs , which exhibited unique hollow and square geometry with the size of 208.1±13 nm as the previous literature reported.[18] After alternately assembling of Sem and AuNPs onto the AuNCs, homogeneous and dense bright dots were covered on the surface of the square structures and the size of $(AuNPs\text{-}Sem)_n$-AuNCs was about 375.8±31 nm (Figure 1F), indicating the adsorption of AuNPs onto the square AuNCs.

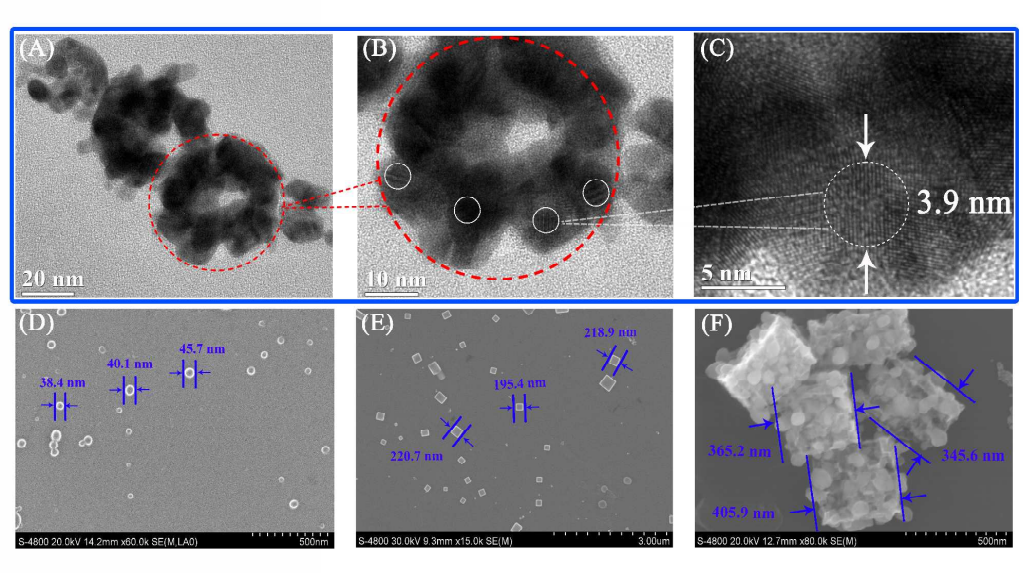

Figure 1. HRTEM images of (A) CdTe QDs@C_{60}NPs composite, (B) an individual CdTe QDs@C_{60}NPs from the enlarged image in (A), (C) a QD with crystalline structure from the enlarged image in (B). SEM images of (D) C_{60}NPs, (E) AuNCs and (F) $(AuNPs\text{-}Sem)_n$-AuNCs.

UV-vis, PL and ECL spectra of CdTe QDs. Firstly, the UV-vis and PL spectra were used to characterize the formation of CdTe QDs. The UV-vis spectrum of the as-prepared CdTe QDs showed an absorption inflection point at 605 nm (Figure 2A, curve *a*). According to Peng's empirical equation,[19] the size of the CdTe QDs was estimated to be 3.7 nm, which was close to the diameters of CdTe QDs measured with the SEM. In the PL spectrum (with excitation wavelength at 400 nm), a strong emission peak was observed at about 632 nm (Figure 2A, curve *b*). The above results were both in agreement with previous report.[20]

Subsequently, we investigated the ECL spectra of the CdTe QD-based ECL systems by using the optical filter technique according to the previously reported methods.[21] Firstly, ECL peak intensity of the detection solutions were collected during the cyclic potential sweep at -1.5~0 V with a series of optical filters at 250~825 nm (spaced 25

nm). Then by means of fitting curves, the continuous and smooth ECL spectra were obtained from the above discontinuous ECL peak values. As we can see from Figure 2B, the ECL spectrum of the QDs+$S_2O_8^{2-}$ solution (where the concentrations of QDs and $S_2O_8^{2-}$ were 0.1 mg/mL and 0.1 M in PBS (pH 7.4), respectively) was detected with the maximum emission wavelength at 650 nm (Figure 2B, curve *a*), which was close to the PL emission spectrum of QDs at 632 nm (Figure 2A, curve *b*) and consistent with the previous literature report.[22] Thus, we could draw a conclusion that QDs were the ECL luminophore and $S_2O_8^{2-}$ was the coreactant in the QDs+$S_2O_8^{2-}$ ECL system. Afterwards, the maximum emission wavelength of the pure $S_2O_8^{2-}$ solution with 0.1 M (Figure 2B, curve *b*) was measured at 575 nm and it could be assigned to the emission of singlet state oxygen ($^1(O_2)_2^*$) in the $O_2/S_2O_8^{2-}$ system.[23] When Sem (0.5 mM) was introduced in the $S_2O_8^{2-}$ solution (0.1 M), the maximum emission wavelength was also at 575 nm (Figure 2B, curve *c*) which was consistent with that of pure $S_2O_8^{2-}$ solution (Figure 2B, curve *b*), suggesting that the two ECL systems (Figure 2B, curve *b* and curve *c*) were both based on the emission of $^1(O_2)_2^*$. Furthermore, the ECL intensity of the $S_2O_8^{2-}$+Sem solution was obviously increased (Figure 2B, curve *c*) compared with the pure $S_2O_8^{2-}$ solution (Figure 2B, curve *b*), indicating that Sem could enhance the ECL signal of the $O_2/S_2O_8^{2-}$ system. Finally, as shown in Figure 2B curve *d*, the maximum emission wavelength of the QDs+$S_2O_8^{2-}$+Sem solution (where the concentrations of QDs, $S_2O_8^{2-}$ and Sem were 0.1 mg/mL, 0.1 M and 0.5 mM respectively) was measured at 650 nm which was consistent with that of QDs+$S_2O_8^{2-}$ solution (Figure 2B, curve *a*). This result implied

that QDs were the luminophore of the QDs+$S_2O_8^{2-}$+Sem ECL system. Notably, the ECL intensity of the QDs+$S_2O_8^{2-}$+Sem solution was improved significantly (Figure 2B, curve *d*) in comparison with the QDs+$S_2O_8^{2-}$ solution (Figure 2B, curve *a*), indicating that Sem could boost the ECL intensity of the QDs+$S_2O_8^{2-}$+Sem ECL system.

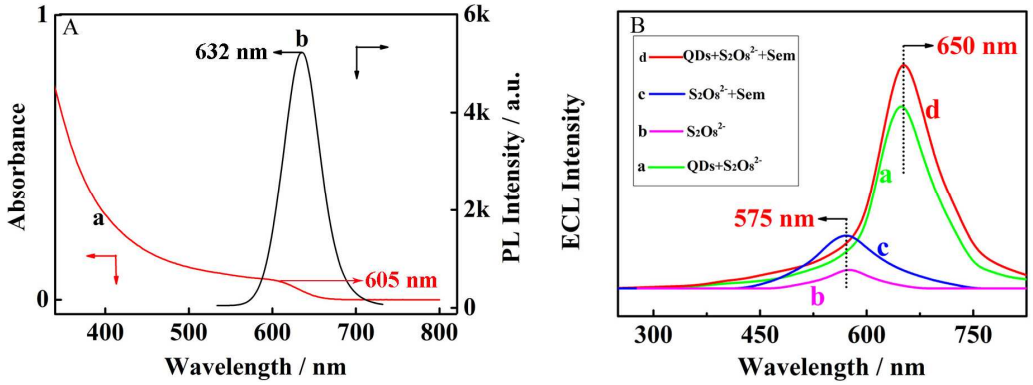

Figure 2. (A) UV–vis (a) and PL (λex = 400 nm) spectra of the CdTe QDs (b). (B) ECL spectra of QDs+$S_2O_8^{2-}$ solution (a), pure $S_2O_8^{2-}$ solution (b), $S_2O_8^{2-}$+Sem solutions (c) QDs+$S_2O_8^{2-}$+Sem solution (d). The concentrations of QDs, $S_2O_8^{2-}$ and Sem were 0.1 mg/mL, 0.1 M and 0.5 mM in PBS (pH 7.4), respectively.

ECL and CV properties. In order to evaluate the possible reaction of CdTe QDs, $S_2O_8^{2-}$ and Sem, we first compared the ECL and CV responses with the GCE in four different solutions of (a) QDs solution, (b) QDs+Sem solution, (c) QDs+$S_2O_8^{2-}$ solution and (d) QDs+ $S_2O_8^{2-}$ +Sem solution (where the concentrations of QDs, $S_2O_8^{2-}$ and Sem were 0.1 mg/mL, 0.1 M and 0.5 mM in PBS (pH 7.4), respectively). The corresponding results were displayed in Figure 3. As shown in Figure 3A, the ECL signal about 400 a.u. was observed in QDs solution (Figure 3A, curve *a*) and it exhibited no remarkable changes in comparison with that in the presence of Sem

(Figure 3A, curve *b*), revealing that Sem had no direct effect on QDs. From the Figure 3A curve *c*, we could see that the ECL signal was noticeably raised to 3700 a.u. when the GCE was measured in QDs+$S_2O_8^{2-}$ solution, which indicated that $S_2O_8^{2-}$ could serve as the coreactant of QDs to improve the ECL response of the QDs+$S_2O_8^{2-}$ ECL system. When Sem was introduced in the QDs+$S_2O_8^{2-}$ ECL system, the highest ECL emission of 5400 a.u. was produced (Figure 3A, curve *d*). This was primarily attributed to the reason that Sem could interact with $S_2O_8^{2-}$ rather than QDs to promote the ECL reaction rate of QDs and $S_2O_8^{2-}$ for significantly boosting the ECL signal of the QDs+$S_2O_8^{2-}$+Sem ECL system.

In addition, to assess the effect of Sem as co-reaction accelerator on the ECL reaction process, we also compared the ECL-Potential curves of GCE in QDs+$S_2O_8^{2-}$ solution with (Figure 3A, curve *d*) and without (Figure 3A, curve *c*) Sem (where the working potential were both set at the -1.5~0 V with the scan rate of 100 mV/s). Firstly, an obvious ECL emission was observed in the QDs+$S_2O_8^{2-}$ solution when the potential was less than -1.14 V (Figure 3A, curve *c*). After Sem was added in the QDs+$S_2O_8^{2-}$ solution, the corresponding potential was positively shifted to -1.08 V (Figure 3A, curve *d*). This phenomenon revealed that the introduction of Sem made the energy of the ECL reaction process of QDs and $S_2O_8^{2-}$ less and let the ECL signal stronger. Furthermore, the inset of Figure 3A showed the ECL-Time curves of GCE in QDs+$S_2O_8^{2-}$ solution with (curve *d*) and without (curve *c*) Sem. We could see that the time took to reach the maximum ECL intensity was faster in the presence of Sem, indicating that Sem as the co-reaction accelerator could actually make the ECL

reaction of QDs and $S_2O_8^{2-}$ more efficient.

Similarly, the CV responses of the four different solutions were also presented in Figure 3B. As shown in Figure 3B curve *a*, a pair of redox peaks of $E_{p,c}$ = -0.88 V and $E_{p,a}$ = -0.65 V could be observed in the QDs solution, which indicated that the reduced form of QDs was stable enough to undergo oxidation on scan reversal.[24] After Sem was added in the QDs solution, the currents and potentials of the redox peaks had no obvious changes (Figure 3B, curve *b*), suggesting that Sem had no direct reaction with QDs. When the GCE was measured in QDs +$S_2O_8^{2-}$ solution, the Figure 3B curve *c* showed a pair of reduction and oxidation peaks of QDs at $E_{p,c}$ = -1.05 V and $E_{p,a}$ = -0.83 V respectively which shifted negatively compared with pure QDs solution (Figure 3B, curve a), owing to the increasing of the overpotential produced by the interaction between $S_2O_8^{2-}$ and QDs. Meanwhile, a new reduction peak at the $E_{p,c}$ = -0.92 V was observed compared with Figure 3B curve *a*, which was corresponded to the reduction of $S_2O_8^{2-}$. When Sem was introduced in the QDs+$S_2O_8^{2-}$ system, the redox peak currents of the QDs were increased and the potentials remained unchanged (Figure 3B, curve *d*). It might be due to the reason that Sem could promote the interaction between QDs and $S_2O_8^{2-}$, thus obtained more QDs at oxidation and reduction states.

Subsequently, in order to study the possible interaction between $S_2O_8^{2-}$ solution and Sem, we compared the CV responses with the GCE in the three different solutions of (a) Sem solution, (b) $S_2O_8^{2-}$ solution and (c) $S_2O_8^{2-}$+Sem solutions (where the concentrations of $S_2O_8^{2-}$ and Sem were 0.1 M and 0.5 mM in PBS (pH 7.4),

respectively). Firstly, it could be seen in the inset of Figure 3B that there were no apparent redox peaks of Sem in the PBS solution (curve *a*) while an obvious reduction peak at -0.94 V was measured in $S_2O_8^{2-}$ solution (curve *b*). When appropriate Sem was added in $S_2O_8^{2-}$ solution, the CV curve (curve *c*) showed one noticeable reduction peak where the reduction potential shifted positively from -0.94V to -0.85 V and the peak current increased, suggesting that Sem made the reduction of $S_2O_8^{2-}$ easier and thus let the oxidant mediators of $SO_4^{\bullet-}$ increase. Furthermore, a current value of -2.35 mA at the potential -2.0 V was observed in the $S_2O_8^{2-}$ solution (curve *b*). After Sem was added in $S_2O_8^{2-}$ solution, the corresponding current value reached to -3.49 mA (curve *c*). This result could be mainly due to the increasing concentration of H^+ on the GCE surface in $S_2O_8^{2-}$+Sem solution. At last, the above results further confirmed that Sem could accelerate the reduction of $S_2O_8^{2-}$ to produce more oxidant mediators of $SO_4^{\bullet-}$.

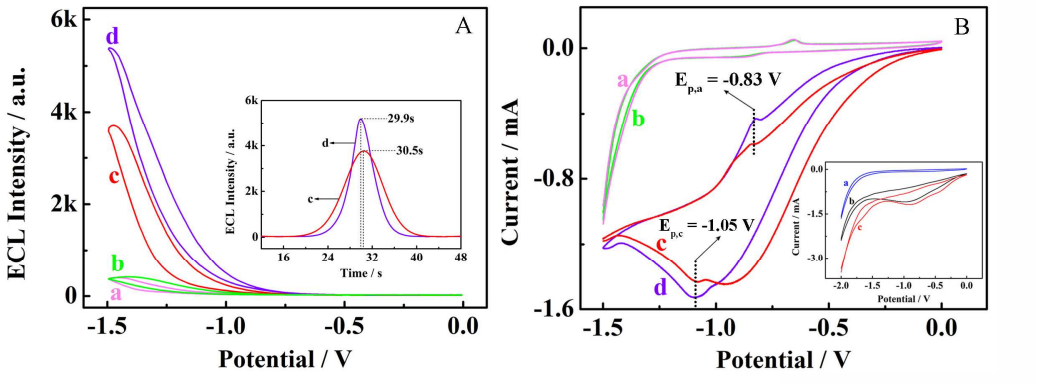

Figure 3. ECL responses (A) and CVs (B) of GCE in (a) QDs solution; (b) QDs+Sem solution; (c) QDs+$S_2O_8^{2-}$ solution and (d) QDs+ $S_2O_8^{2-}$+Sem solution. Inset of (A): ECL-Time curves of bare GCE in QDs+$S_2O_8^{2-}$ solution with (curve *d*) and without (curve *c*) Sem. Inset of (B): CV curves of bare GCE in (a) Sem solution, (b) $S_2O_8^{2-}$ solution and (c) $S_2O_8^{2-}$+Sem solutions, respectively. The

concentrations of QDs, $S_2O_8^{2-}$ and Sem were 0.1 mg/mL, 0.1 M and 0.5 mM in PBS (pH 7.4), respectively.

The possible ECL mechanisms of different ECL systems. Supported by the above experimental results, we could see that Sem was indeed defined as the co-reaction accelerator to interact with $S_2O_8^{2-}$ rather than QDs for promoting the ECL reaction rate of QDs and $S_2O_8^{2-}$, thus significantly boosted the ECL signal of the QDs+$S_2O_8^{2-}$+Sem system. The possible ECL mechanisms of O_2/$S_2O_8^{2-}$, O_2/$S_2O_8^{2-}$+Sem, QDs+$S_2O_8^{2-}$ and QDs+$S_2O_8^{2-}$+Sem systems were shown as follows (Scheme 2). Briefly, when the GCE was measured in pure $S_2O_8^{2-}$ solution and QDs+$S_2O_8^{2-}$ solution without Sem, the oxidant mediators of $SO_4^{\bullet-}$ were obtained only through the electron exchange of $S_2O_8^{2-}$ on the GCE surface (Scheme 2 (a) and (c), Route ①). However, when Sem was introduced in the above two solutions, the amount of oxidant mediators of $SO_4^{\bullet-}$ could increase significantly due to the following two reaction routes (Scheme 2 (b) and (d), Route ① and ②). ① Electron exchange of $S_2O_8^{2-}$ on the GCE surface to generate $SO_4^{\bullet-}$; ② Interaction between $S_2O_8^{2-}$ and Sem$^{\bullet}$ produced by the electron exchange on the GCE surface to generate $SO_4^{\bullet-}$. Therefore, the employment of Sem made the ECL reaction easier and more efficient.

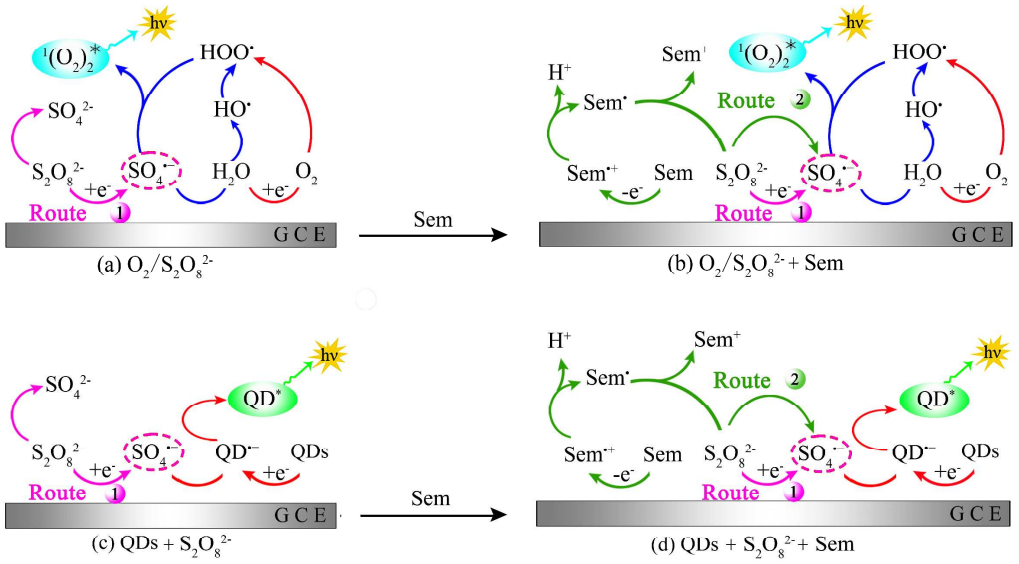

Scheme 2. The possible ECL mechanisms of (a) $O_2/S_2O_8^{2-}$ system; (b) $O_2/S_2O_8^{2-}$+Sem system; (c) QDs+$S_2O_8^{2-}$ system and (d) QDs+$S_2O_8^{2-}$+Sem system.

ECL characterization of stepwise fabrication of the aptasensor. The ECL characterizations of the stepwise fabrication process of the aptasensor were performed in $S_2O_8^{2-}$ solution (0.1 M, pH = 7.4). As shown from the ECL dynamic curve (Figure 4A) and ECL-potential curve (Figure 4B), a low ECL response was observed with the bare GCE (curve *a*), since no QDs existesd in the testing buffer containing $S_2O_8^{2-}$. After CdTe QDs@C_{60}NPs composite was dropped on the electrode, the ECL intensity was enhanced apparently (curve *b*), for that $S_2O_8^{2-}$ could serve as the coreactant of the CdTe QDs@C_{60}NPs composite to improve the ECL response. When Dp AuNPs was electrodeposited onto the electrode surface, the ECL signal was further improved (curve *c*), indicating Dp AuNPs could promote the electron transfer in ECL reaction process.[25] A decrease in ECL intensity was observed after TBA 1 (curve *d*) was immobilized on the electrode. Subsequently, the electrode was blocked with BSA

(curve *e*) and incubated with TB (curve *f*), the ECL responses were further decreased. These decreases could be mainly due to the reason that TBA 1, BSA and TB were all kinds of non-electroactive micromolecule, which could dramatically increase the steric hindrance and obstruct the electron transfer tunnel of the electrode surface. Meanwhile, to further confirm the fabrication process of the ECL aptasensor, CV and EIS were also carried out in 5 mM $[Fe(CN)_6]^{3-/4-}$ solution (see Figure S1, Supporting Information). In addition, the experimental conditions of the working potential of CdTe QDs and the adsorption layers of AuNPs and Sem were both optimized in this experiment (Figure S2, Supporting Information).

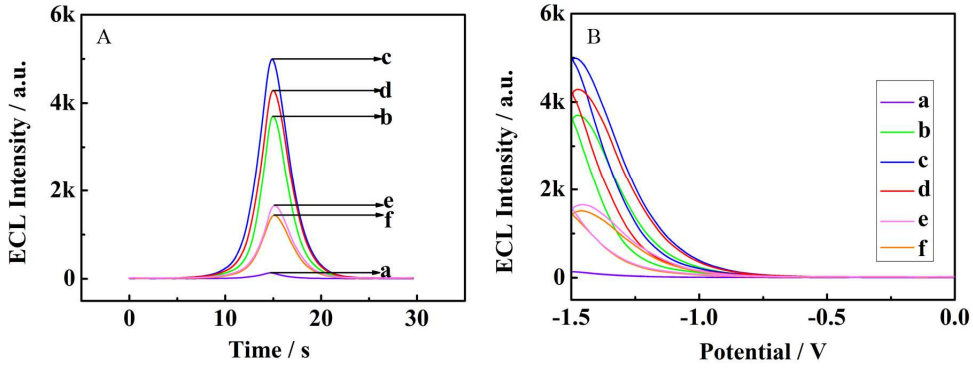

Figure 4. ECL dynamic curve (A) and ECL-potential curve (B) of differently modified electrodes in 0.1 M $S_2O_8^{2-}$ solution: (a) bare GCE; (b) CdTe QDs@C_{60}NPs/GCE; (c) Dp AuNPs/CdTe QDs@C_{60}NPs/GCE; (d) TBA 1/Dp AuNPs/CdTe QDs@C_{60}NPs/GCE; (e) BSA/TBA 1/Dp AuNPs/CdTe QDs@C_{60}NPs/GCE and (f) TB/BSA/TBA 1/Dp AuNPs /CdTe QDs@C_{60}NPs/GCE.

Comparison of the ECL responses with different TBA 2 signal probes. Under the optimized experimental conditions, four kinds of different TBA 2 signal probes were prepared to investigate the amplification properties. They were the proposed probe *D* of TBA 2-(AuNPs-Sem)$_2$-AuNCs and the compared probe *A* of TBA

2-AuNCs, probe *B* of TBA 2-Sem-AuNCs and probe *C* of TBA 2-AuNPs-Sem-AuNCs. Then the aptasensors with the same batch were incubated with the same concentration TB of 0.1 nM, followed by incubating with the above four kinds of TBA 2 signal probes, respectively. Afterwards, the resultant aptasensors were all measured in 0.1 M $S_2O_8^{2-}$ solutions by comparing their ECL responses. As shown in Figure 5, the curve *a*, *b*, *c* and *d* exhibited the ECL intensity of the aptasensor after immobilizing of different TBA 2 signal probes and curve *e* displayed the ECL signal of the aptasensor before incubating with TB. When probe *A* was incubated on the aptasensor, the ECL signal of the aptasensor was slightly decreased compared with that of curve *e* (curve *a*) and it was primarily due to two facts. First, the materials in probe *A* could not enhance the ECL intensity. Second, the formation of sandwich-type structure of the TBA 1, TB and probe *A* might hinder the diffusion of corectant toward the electrode surface. After probe *B* was captured on the aptasensor (curve *b*), the ECL response was increase slightly to 2493 a.u, for that the employment of Sem as co-reaction accelerator into the TBA 2 signal probe could enhance the ECL intensity. However, owing to the limited immobilization amount of Sem and the depressed reactivity of Sem caused by the crosslinking effect of Sem with TBA 2 *via* GA, the ECL response was increase slightly. Subsequently**,** when probe *C* was incubated on the aptasensor, a higher ECL intensity of 3702 a.u was observed (curve *c*) compared with curve *b*, and it was primarily due to the fact that Sem maintained the reactivity through self assembly of -NH_2 terminal groups onto the surface of AuNCs. Notably, when the proposed probe *D* of TBA

2-(AuNPs-Sem)$_2$-AuNCs was incubated on the aptasensor, the ECL response was remarkably raised to 9094 a.u (curve *d*) for that numerous co-reaction accelerator Sem involved in probe *D*. Therefore, the proposed probe of TBA2-(AuNPs-Sem)$_2$-AuNCs was proved to boost the ECL signal significantly and it was mainly attributed to the amplified effect of Sem as co-reaction accelerator toward the QD-based ECL system.

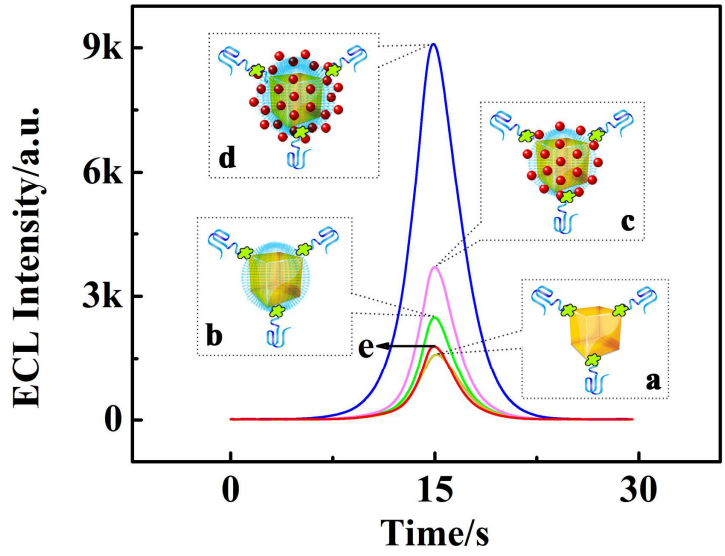

Figure 5. The ECL responses of aptasensors using different signal probes: (a) probe *A* of TBA 2-AuNCs; (b) probe *B* of TBA 2-Sem-AuNCs; (c) probe *C* of TBA 2-AuNPs-Sem-AuNCs and (d) probe *D* of TBA2-(AuNPs-Sem)$_2$-AuNCs. (e) ECL signal of the aptasensor before reacting with TB.

The calibration curve for TB detection. Under the optimal experimental conditions, quantitative analysis of the TB concentration was based on the ΔI_{ECL} ($\Delta I_{ECL} = I - I_0$, I was the ECL intensity of the aptasensor after immobilizing of TBA 2 signal probes and I_0 was the ECL intensity of the aptasensor before incubating with TB, respectively) of the CdTe QD-based ECL system. It could be seen from Figure 6 that ΔI_{ECL} linearly increased as the concentration of TB increased from 1×10^{-7} nM to 1

nM. The linear regression equation was ΔI_{ECL} =1210.6 lg c + 8523.7 (where c indicated the concentration of TB) with a correlation coefficient of 0.9972 and detection limit of 0.03 fM (S/N=3). Compared with other reported sensors based on different ECL systems for TB detection (Table 1), the designed aptasensor with TBA 2-(AuNPs-Sem)$_2$-AuNCs as signal probe showed a wider linear range and a lower detection limit for detecting TB concentration quantitatively.

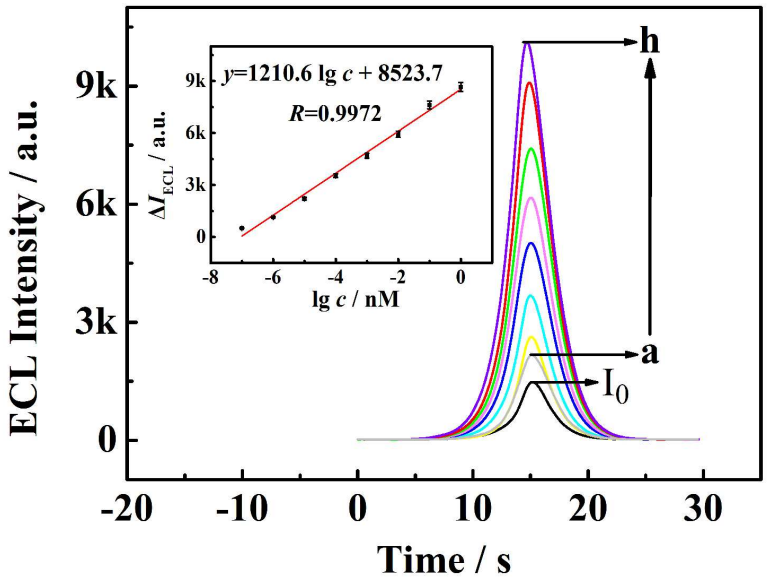

Figure 6. ECL intensity of the aptasensors with different TB concentrations. TB concentration: (a) 1×10^{-7} nM, (b) 1×10^{-6} nM, (c) 1×10^{-5} nM, (d) 1×10^{-4} nM, (e) 1×10^{-3} nM, (f) 0.01 nM, (g) 0.1 nM, (h) 1 nM. Inset: calibration curve for TB detection. $\Delta I_{ECL} = I - I_0$, I was the ECL intensity of the aptasensor after immobilizing of TBA 2 signal probes and I_0 was the ECL intensity of the aptasensor before incubating with TB, respectively.

Table 1. Comparison of the TB detection with different ECL systems.

ECL system	Linear range	LOD	Ref.
Fe_3O_4@CdSe/$S_2O_8^{2-}$	1.0 pM–5.0 nM	0.12 pM	26

$CdS/S_2O_8^{2-}$	1.0 fM –100 fM	—	27
$CdTe/S_2O_8^{2-}$	0.5 pM–800 pM	0.35 pM	28
$CdSe\text{-}ZnS/S_2O_8^{2-}$	27.2 nM–545 nM	2.72 nM	29
$CdTe/S_2O_8^{2-}$/Sem	0.1 fM–1.0 nM	0.03 fM	Present work

Selectivity and stability of the aptasensor. The selectivity of our proposed aptasensor for TB detection was investigated by using the interferences of HSA and Hb. It could be observed from Figure 7A that the presence of TB (0.1 nM) produced much higher ECL response compared with that of the interference molecules of 1 nM HSA and 1 nM Hb respectively. This phenomenon suggested that the proposed aptasensor exhibited high selectivity toward TB. Then the proposed aptasensor was incubated with 1×10^{-5} nM TB and cyclic scanned in 0.1 M $S_2O_8^{2-}$ solution to monitor its stability. As shown in Figure 7B, the 8 measurements of the electrode exhibited a coincident ECL response with an RSD of 0.92%, revealing the acceptable stability for TB detection. In addition, the preliminary analysis of real TB samples with the proposed aptasensor was also carried out and results of recovery experiments were listed in Table S1, Supporting Information.

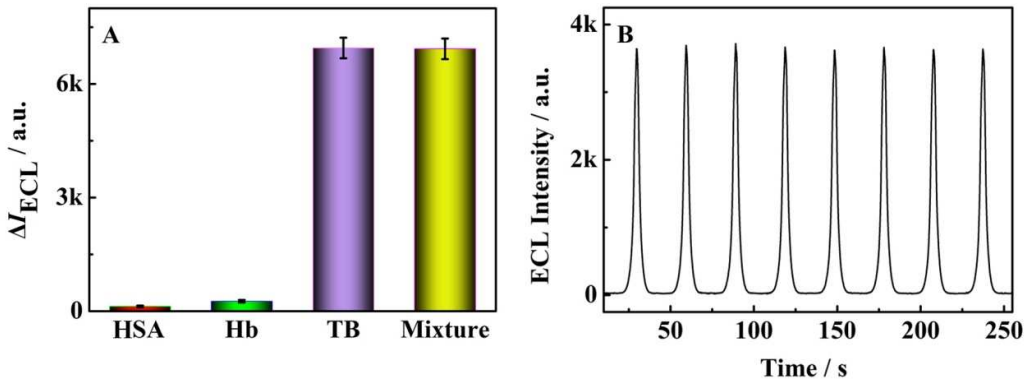

Figure 7. (A) The selectivity of the proposed aptasensor against different samples: (a) 1 nM HSA;

(b) 1 nM Hb; (c) 0.1 nM TB and (d) 1 nM HSA+1 nM Hb+0.1 nM TB. (B) The ECL stability of the aptasensor toward 1×10^{-5} nM TB based on continuous cyclic scanning in 0.1 M $S_2O_8^{2-}$ solution.

CONCLUSIONS

In conclusion, to improve the ECL efficiency of the aptasensor, a new signal amplification strategy based on the employment of Sem as co-reaction accelerator to promote the ECL reaction rate of CdTe QDs and $S_2O_8^{2-}$ for boosting signal amplification was first proposed. Herein, the Sem could interact with $S_2O_8^{2-}$ to produce the more oxidant mediators of $SO_4^{\bullet-}$, which further enhanced the production of excited states of CdTe QDs to emit light. In view of this, a kind of multi-layered nanomaterials of $(AuNPs\text{-}Sem)_2$-AuNCs was prepared as signal label to construct an ECL aptasensor which utilized TB as the experimental model to achieve a wide linear range, low detection limit, good stability and high selectivity for TB detection. Therefore, this method based on the employment of Sem as co-reaction accelerator for boosting the ECL intensity was simple, efficient, and low-cost, which held a new perspective for signal amplification of ECL biosensing.

ASSOCIATED CONTENT

Supporting Information

Additional information as described in text. This material is available free of charge via the Internet at http://pubs.acs.org/.

AUTHOR INFORMATION

*** Corresponding authors**

Tel.: +86 23 68252277, fax: +86 23 68253172.

E-mail addresses: yingzhuo@swu.edu.cn (Y. Zhuo), yqchai@swu.edu.cn (Y.Q.Chai).

Notes

The authors declare no competing financial interest.

ACKNOWLEDGMENT

This research was supported by the NNSF of China (21575116, 51473136, 21275119, 21105081), and the Fundamental Research Funds for the Central Universities (XDJK2015A002, XDJK2014A012), China.

REFERENCES

(1) Ding, Z.F.; Quinn, B.M.; Haram, S.K.; Pell, L.E.; Korgel, B.A.; Bard, A.J. *Science*, **2002**, 296, 1293.

(2) Medintz, I.L.;Uyeda, H.T.;Goldman, E.R.; Mattoussi, H. *Nat. Mater.,* **2005**, 4, 435-446.

(3) Zhao, W.W.; Han, Y.M.; Zhu, Y.C.; Zhang, N.; Xu, J.J.; Chen, H.Y. *Anal. Chem.*, **201**5, 87, 5496–5499.

(4) Wu, K.F.; Zhu, H.M.; Lian, T.Q. *Acc. Chem. Res.*, **2015**, 48, 851−859.

(5) Lin,X.M.; Luo, F.Q.; Zheng, L.Y.; Gao, G.M.; Chi, Y.W. *Anal. Chem.*, **2015**, 87, 4864–4870.

(6) Hu, L.Z.; Xu, G.B. *Chem. Soc. Rev.*, **2010**, 39, 3275-3304.

(7) Yu, Y.C.; Lu, C.; Zhang, M.N. *Anal. Chem.*, **2015**, 87, 8026 − 8032.

(8) Jie, G.B.; Pan, L.H.; Zhu, J.J.; Chen, H.Y. *Anal. Chem.*, **2007**, 79, 5574–5581.

(9) Liu, S.F.; Zhang, X.; Yu, Y.M.; Zou, G.Z. *Anal. Chem.*, **2014,** 86, 2784–2788.

(10) Lei, J.P.; Ju, H.X. *Trends Anal. Chem.*, **2011**, 30, 1351-1359.

(11) Skrabalak, S.E.; Chen, J.Y.; Sun, Y.G.; Lu, X.M.; Au, L.; Cobley, C.M.; Xia, Y.N. *Acc. Chem. Res.*, **2008**, 41, 1587-1595.

(12) Zheng, T.T.; Zhang, Q.F.; Feng, S.; Zhu, J.J.; Wang, Q.; Wang, H. *J. Am. Chem. Soc.*, **2014**, 136, 2288–2291.

(13) Au, L.; Chen, Y.C.; Ginger, D.S.; Xia, Y.N. *Nano Res*., **2008**, 1, 441 449.

(14) Andrievsky, G.V.; Kosevich, M.V.; Vovk, O.M.; Shelkovsky, V.S.; Vashchenko, L.A. *J. Chem. Soc., Chem. Commun.*, **1995**, 12, 1281-1282.

(15) Enustun, B.V.; Turkevich, J. J. *J. Am. Chem. Soc.*, **1963**, 85, 3317.

(16) Huang, K.; Xu, K.L.; Tang, J.; Yang, L.; Zhou, J.R. Hou, X.D.; Zheng, C.B.

Anal. Chem., **2015,** 87, 6584–6591.

(17) Li, H.L.; Zhai, J.F.; Sun, X.P. *Nanoscale*, **2011**, 5, 2155-2157.

(18) Gao, L.; Fei, J.B.; Zhao, J.; Li, H.; Cui, Y.; Li, J.B. *ACS nano*, **2012**, 6, 8030–8040.

(19) Yu, W.W.; Qu, L.H.; Guo, W.Z.; Peng, X.G. *Chem. Mater.*, **2003**, 15, 2854-2860.

(20) Duan, J.L.; Song, L.X.; Zhan, J.H. *Nano Res.*, **2009**, 2, 61-68.

(21) Li, L.L.; Ji, J.; Fei, R.; Wang, C.Z.; Lu, Q.; Zhang, J.R.; Jiang, L.P.; Zhu, J.J. *Adv. Funct. Mater.*, **2012**, 22, 2971–2979.

(22) Myung, N.; Lu, X.M.; Johnston, K.P.; Bard, A.J. *Nano Lett.*, **2004**, 4, 183-185.

(23) Yao, W.; Wang, L.; Wang, H.Y.; Zhang, X.L. *Electrochim. Acta*, **2008**, 54, 733–737.

(24) Shan, Y.; Xu, J.J.; Chen, H.Y. *Chem.Commun.*, **2009**, 905, 905–907.

(25) Cui, H.; Wang, W.; Duan, C.F.; Dong, Y.P.; Guo, J.Z. *Chem.-Eur.J.*, **2007**, 13, 6975-6984.

(26) Jie, G.F.; Yuan, J.X. *Anal. Chem.*, **2012**, 84, 2811–2817.

(27) Guo, Y.S.; Jia, X.P.; Zhang, S.S. *Chem. Commun.*, **2011**, 47, 725–727.

(28) Chen, Y.; Jiang, B.Y.; Xiang, Y.; Chai, Y.Q.; Yuan, R. *Chem.Commun.*, **2011**, 47, 7758–7760.

(29) Huang, H.P.; Zhu, J.J. *Biosens. Bioelectron.*, **2009**, 25, 927–930.

For TOC only

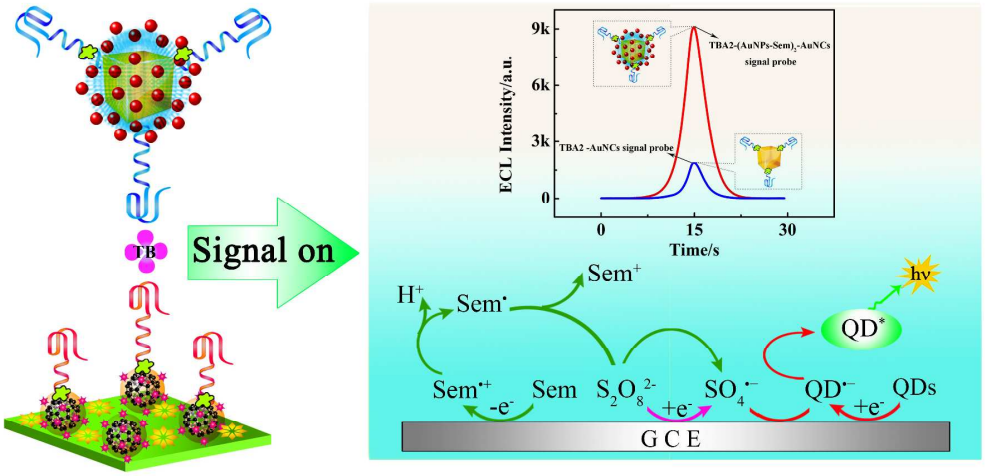
TB
Signal on
ECL Intensity/a.u.
Time/s
TBA2-(AuNPs-Sem)2-AuNCs signal probe
TBA2 -AuNCs signal probe
H+
Sem•
Sem+
Sem•+
Sem
S2O8 2-
SO4 •−
QD*
QD•−
QDs
hv
-e-
+e-
+e-
G C E